

# Density functional theory for a macroion suspension

Patrick B. Warren

*Unilever R&D Port Sunlight, Bebington, Wirral, CH63 3JW, UK.*

(Dated: June 9, 2005)

A density functional theory for a macroion suspension is examined, where the excess free energy corresponds to the macroion self energy arising from the polarisation of the supporting electrolyte solution. This is treated within a linearised or Debye-Hückel approximation. The model predicts liquid-liquid phase separation at low ionic strength. The interface structure and surface tension between coexisting phases is calculated using a variational approximation. Results are also obtained for structure factors, which are shown to obey the Stillinger-Lovett moment conditions. As one approaches the critical points, the structure factors may diverge at a non-zero wavevector, indicating that the critical points could be replaced by charge-density-wave phases.

## I. INTRODUCTION

The phase behaviour of charged colloidal suspensions at low ionic strength has attracted much experimental and theoretical interest. Observations of void structures and other phenomena [1, 2] motivated a number of theoretical studies which attributed the anomalous behaviour to phase separation between colloid-rich and colloid-poor phases [3, 4, 5, 6]. Several reviews are available [7, 8]. The original theoretical explanations have come under strong attack for using a Debye-Hückel linearisation approximation which is, at best, at the margin of its validity. Various attempts to patch this up have left the situation unclear. Cell model calculations using Poisson-Boltzmann theory indicate the original predictions are an artefact of the linearisation approximation [9, 10]. The Debye-Hückel approximation can be improved by taking into account counterion condensation, in which case the phase transition may or may not be recovered depending on the approximation scheme used [11]. Other approaches such as extended Debye-Hückel theory [12], symmetrised Poisson-Boltzmann theory [13, 14], ‘bootstrap’ Poisson-Boltzmann theory [15], and a systematic expansion into two- and three-body interactions [16, 17], all indicate that a phase transition can occur, as do several integral equation studies [18, 19]. The experimental situation is also uncertain since a plausible alternative explanation has been suggested [8], in which the voids correspond to regions occupied by dilute, highly extended (and therefore effectively invisible) polyelectrolyte chains which have been shed by the latex colloids.

Simulation methods struggle to approach these problems because of the disparity in size between the macroions and the small ions, and the need to handle the electrostatic interactions. Nevertheless, convincing evidence has been found for liquid-liquid phase separation in a macroion system at lower dimensionless temperatures [20, 21]. Experimentally this corresponds to a solvent with a lower dielectric constant than water (but one in which the ions still disperse). Charged colloids in such solvents exhibit many interesting phenomena [22].

Thus, whilst the weight of evidence perhaps suggests that aqueous charge-stabilised colloidal suspensions may

not show genuine liquid-liquid phase coexistence, it is absolutely clear that there will be phase coexistence between condensed and dilute colloidal phases at small enough dimensionless temperatures. In this sense, the problem resembles the much-studied restricted primitive model (RPM), whose phase behaviour is now well established [23, 24, 25, 26].

In situations where genuine phase coexistence obtains, one can go on to ask questions about the surface tension and electrical structure of the interface between the coexisting phases. Answers to these questions may prompt new avenues for experimental investigation of real systems. Previously, Knott and Ford compute the surface tension using square-gradient theory, but discard the possible electrical structure at the interface [27]. The present work approaches this problem within the context of a density functional theory, motivated by the earlier study in Ref. [5] (see also Appendix A). It places the phenomenological remarks made in this earlier work on a sounder footing. The analysis in Ref. [5] suggests that the macroion self energy is the dominant contribution to the excess free energy, similar to an early insight by Langmuir [28]. In the present work therefore, the rather gross simplification has been adopted in which the macroion self energy is the *only* contribution to the excess free energy. Moreover this self energy is computed in a simple closed form using Debye-Hückel theory, and is thus also based on the much-criticised linearisation approximation. Nevertheless I argue that it is instructive to proceed, because of the rich phenomenology that is revealed.

The model predicts phase separation at low dimensionless temperatures and low ionic strengths, and in quantitative terms stands reasonable comparison with some of the other approaches. The physics of the phase separation lies in the dependence of the macroion self energy on the local ionic strength: macroions drift towards regions of high ionic strength, which by charge neutrality are regions where other macroions have also congregated. Within the linearisation approximation, the effect grows without bound as the macroion charge is increased, and thus the mechanism can drive phase separation at sufficiently large macroion charges. In reality, non-linear effects (counterion condensation) limit the effective macroion charge [29], and therefore this mecha-

nism is probably insufficient in itself to drive phase separation in real systems. Undoubtedly though it is still a contributing factor, operating in conjunction with other effects such as correlated fluctuations in the counterion clouds around macroions and the sharing of counterions between macroions [2, 20, 30].

The model is constructed in the form of a density functional theory. Thus, as well as making predictions for phase separation, it can be used to solve for the density profiles and the surface tension between coexisting phases. The results obtained here are in accord with typical expectations for soft condensed matter systems [31], and were summarised in an earlier publication [32]. In addition, I also discuss the predictions that the theory makes for the structure factors. These are found to obey the Stillinger-Lovett moment conditions [33, 34], although it turns out this is not a stringent test of the theory. Intriguingly, I find that the structure factors may diverge at a non-zero wavevector as one approaches the critical points. This suggests the possibility that the critical points in these systems may be replaced by charge-density-wave phases [35]. This phenomenological possibility in charged systems was first suggested by Nabutovskii and coworkers [23, 36, 37].

## II. SPECIFICATION OF THE MODEL

The underlying model of the macroion suspension used here is a primitive model commonly deployed for this kind of problem. The ‘primitive’ aspect is that the solvent is treated as a structureless dielectric continuum in which the macroions and small salt ions are embedded. The macroions are treated as spheres of (positive) charge  $Z$ , diameter  $\sigma$ , and number density  $\rho_m$  (volume fraction  $\phi = \pi\sigma^3\rho_m/6$ ). The salt ions are univalent counterions and coions at number densities  $\rho_-$  and  $\rho_+$  respectively. I suppose there is only one species of counterion. The size of the salt ions is assumed to be small enough to be irrelevant. The dielectric continuum is characterised by a Bjerrum length  $l_B$  so that the electrostatic interaction energy between a pair of univalent charges separated by a distance  $r$  is  $l_B/r$ , in units of  $k_B T$  where  $k_B$  is Boltzmann’s constant and  $T$  is the temperature. For water at room temperature,  $l_B \approx 0.72$  nm. The model is completely parametrised by the dimensionless ratio  $\sigma/l_B$  and the charge  $Z$ . It is often convenient to pretend that the dielectric permittivity of the background is independent of temperature, in which case  $l_B \sim 1/T$ . This means that  $\sigma/l_B$  can be regarded as a dimensionless temperature.

The density functional theory is specified by giving the free energy  $F$  as a functional of the spatially varying number densities  $\rho_m(\mathbf{r})$  and  $\rho_{\pm}(\mathbf{r})$  [38]. The functional is decomposed into ideal, mean-field, and correlation con-

tributions:

$$\begin{aligned} \frac{F}{k_B T} = & \int d^3\mathbf{r} \sum_{i=m,\pm} \rho_i(\mathbf{r}) \ln \frac{\rho_i(\mathbf{r})}{e\rho_i^\ominus} \\ & + \frac{l_B}{2} \int d^3\mathbf{r} d^3\mathbf{r}' \frac{\rho_z(\mathbf{r})\rho_z(\mathbf{r}')}{|\mathbf{r}-\mathbf{r}'|}, \\ & + \frac{1}{k_B T} \int d^3\mathbf{r} \rho_m(\mathbf{r}) f_m(\mathbf{r}). \end{aligned} \quad (1)$$

The first term is the ideal term:  $e$  is the base of natural logarithms and the  $\rho_i^\ominus$  are unimportant base units of concentration related to the definition of the standard state [39]. The second term is a mean-field electrostatics term:  $\rho_z(\mathbf{r}) = \sum_i z_i \rho_i(\mathbf{r})$  is the local charge density with  $z_i = \{Z, 1, -1\}$  as  $i = \{m, +, -\}$ , and a factor  $1/2$  allows for double counting. The third term (correlation term) represents the excess free energy. As discussed above, only the macroion self energy  $f_m$  is included in this term. This is computed using Debye-Hückel theory [4, 40, 41, 42],

$$f_m(\mathbf{r}) = \frac{2Z^2 l_B k_B T}{\sigma(\sigma\kappa(\mathbf{r}) + 2)}, \quad (2)$$

where  $\kappa(\mathbf{r})$  is a local inverse Debye screening length. This is defined in terms of an *average* local ionic strength,  $\bar{\rho}_I(\mathbf{r})$ , through

$$\begin{aligned} [\kappa(\mathbf{r})]^2 &= 8\pi l_B \bar{\rho}_I(\mathbf{r}), \\ \bar{\rho}_I(\mathbf{r}) &= \int d^3\mathbf{r}' w(|\mathbf{r}-\mathbf{r}'|) \rho_I(\mathbf{r}') \\ \rho_I(\mathbf{r}') &= [\rho_+(\mathbf{r}') + \rho_-(\mathbf{r}')]/2. \end{aligned} \quad (3)$$

The ionic strength includes the counterions and salt ions, but not the macroions. In principle, allowance should be made for the macroion excluded volume, but this effect is of secondary importance and for simplicity has been omitted.

The smoothing kernel in the second of Eqs. (3) is normalised so that  $\int d^3\mathbf{r} w(r) = 1$ . Here I use

$$w(r) = (\pi\alpha\sigma^2)^{-3/2} \exp[-r^2/(\alpha\sigma^2)]. \quad (4)$$

This is an arbitrarily chosen function [43], of range  $\alpha^{1/2}\sigma$ . The argument below suggests that the parameter  $\alpha$  should be of order unity and for the most part I will set  $\alpha = 1$  in the calculations. Eqs. (1)–(4) completely specify the density functional theory, and everything discussed below can be derived from them.

The decomposition into ideal, mean field, and correlation contributions is a standard approach [44, 45, 46]. The approximation made for the correlation term deserves more discussion though. The only piece of physics that has been incorporated is the macroion self energy. This has a non-trivial dependence on the local ionic strength since each macroion polarises the surrounding electrolyte and becomes surrounded by a ‘double layer’.

This dependence causes macroions to drift towards regions of high ionic strength, as discussed already.

The physical reason for introducing a smoothing kernel is that one can derive the self energy by integrating over the small ion degrees of freedom, with the main contribution coming from variations on length scales corresponding to the structure in the double layer [4]. Thus only variations in ionic strength on length scales  $\gtrsim \sigma$  should be included in the model. The smoothing kernel is a device for achieving this. This argument also motivates the choice for  $\alpha$  in Eq. (4).

In section V below, it is found that the theory is not well behaved if one uses a ‘point model’ where the dependence is on the ionic strength at, say, the centre of the macroion (the first of Eqs. (3) with  $\bar{\rho}_I$  replaced by  $\rho_I$ ). This provides a second technical reason to make the self energy depend on a smeared ionic strength.

The potential energy of a small ion at the surface of the macroion, in units of  $k_B T$ , is  $\pm Z l_B / \sigma$ . Eq. (2) uses the Debye-Hückel expression for the self energy, which assumes  $Z l_B / \sigma \ll 1$ . The expression becomes increasingly inaccurate for  $Z l_B / \sigma \gtrsim 1$ , and its use has been the subject of strong criticism as discussed above. Since the interesting effects are found only at larger values of  $Z l_B / \sigma$ , one should interpret the quantitative results with caution.

### III. BULK PHASE BEHAVIOUR

In this section, I shall consider the bulk phase behaviour predicted by the free energy of Eqs. (1)–(4). This is a homogeneous situation in which the density variables lose their spatial dependence. In this limit, one can prove that the mean field term should be replaced by a condition of bulk charge neutrality,  $\rho_z = \sum_i z_i \rho_i = 0$  [10, 47].

The required charge neutrality condition can be imposed in two ways. The first route is to add a term  $\psi k_B T \sum_i z_i \rho_i$  to the free energy, where  $\psi k_B T$  is a Lagrange multiplier. This approach has the advantage of making a close connection to the density functional theory. Taking this approach, the free energy becomes

$$\frac{F}{V k_B T} = \sum_i \rho_i \left( \ln \frac{\rho_i}{e \rho_i^*} + z_i \psi \right) + \frac{2Z^2 l_B \rho_m}{\sigma(\sigma \kappa + 2)} \quad (5)$$

where  $V$  is the system volume and  $\kappa^2 = 4\pi l_B (\rho_+ + \rho_-)$ . The distinction between the smoothed and unsmoothed ionic strength disappears in the homogeneous limit. In this approach the  $\rho_i$  are treated as three independent density variables. At the end of any calculations,  $\psi$  is adjusted to get  $\sum_i z_i \rho_i = 0$ . The value of  $\psi$  depends on the state point under consideration.

The second way to enforce charge neutrality is to eliminate one of the density variables. Since this is numerically quite convenient, it is the approach that shall be adopted in the rest of this section. At this point one can recognise that the coions come from added salt and

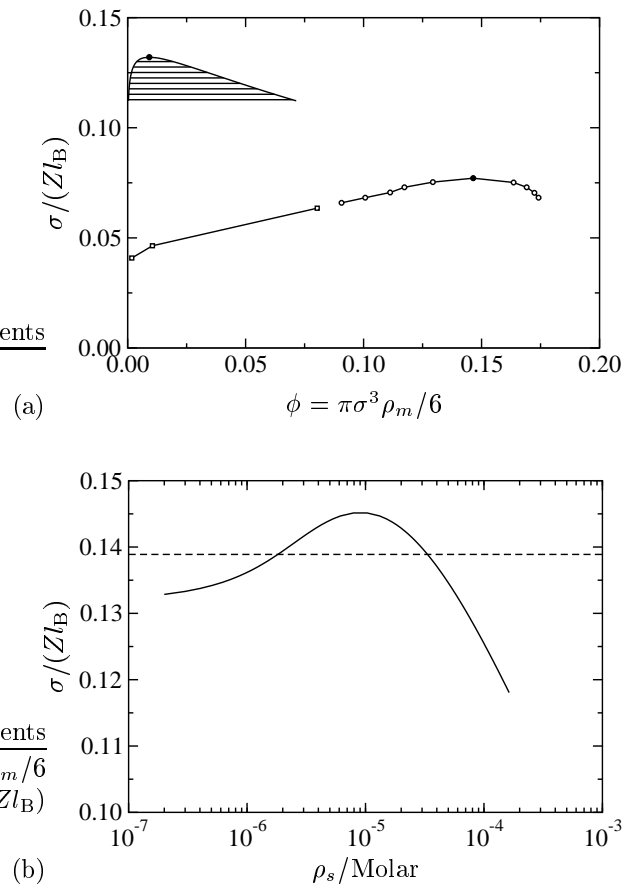


FIG. 1: (a) Universal phase behaviour in the absence of salt, predicted by Eq. (6) (upper curve). The simulation results of Reščič and Linse [21] are also shown (lower curve with marked points). (b) Behaviour of the critical point at  $Z = 10^3$  as salt is added. The dashed line corresponds to the parameters used in Fig. 2.

write  $\rho_- = Z \rho_m + \rho_s$  and  $\rho_+ = \rho_s$ , where  $\rho_s$  is the added salt concentration. The free energy is given by Eq. (5) but with  $\psi = 0$ , and  $\rho_{\pm}$  substituted by the above expressions. There are now only two independent density variables and the phase behaviour can be represented in the  $(\rho_m, \rho_s)$  plane.

I now discuss the phase behaviour predicted by this free energy. Firstly, in the absence of salt some additional simplifications can be made. In the limit  $\rho_s \rightarrow 0$ , the free energy can be written in a dimensionless form as

$$\frac{\pi \sigma^3 F}{6ZV k_B T} = \phi \ln \phi + \frac{2\phi Z l_B / \sigma}{(24\phi Z l_B / \sigma)^{1/2} + 2} \quad (6)$$

where  $\phi$  is the macroion volume fraction. To get to this point, I have assumed that  $Z \gg 1$  and hidden some constants and terms strictly proportional to  $\rho_m$  since they do not affect the phase behaviour.

Eq. (6) predicts the dependence on  $\sigma/l_B$  and  $Z$  is through the single combination  $Z l_B / \sigma$  (there is no reason to suppose that this should be the case in a more

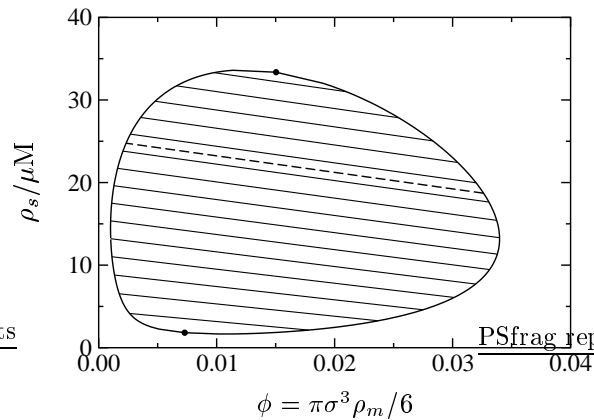


FIG. 2: Phase behaviour at  $Z = 10^3$ ,  $\sigma = 100$  nm and  $l_B = 0.72$  nm, corresponding to the dashed line in Fig. 1. The miscibility gap is bounded above and below by critical points. The dashed tie line is the one for which the interfacial properties are reported in Figs. 3–5.

accurate theory). This is the same parameter that quantifies the accuracy of the Debye-Hückel linearisation approximation. The inverse of this,  $\sigma/(Zl_B)$ , is proportional to the dimensionless temperature discussed above. Fig. 1(a) shows the universal phase behaviour predicted by Eq. (6) as a function of the macroion volume fraction and  $\sigma/(Zl_B)$ . At small enough values of  $\sigma/(Zl_B)$ , a two phase region is encountered in the phase diagram. The two phase region corresponds to phase coexistence between macroion rich and macroion poor phases. The identities of these phases merge at a critical point located at  $\phi \approx 9.18 \times 10^{-3}$  and  $\sigma/(Zl_B) \approx 0.132$ .

One can compare this with the simulation results of Reščič and Linse for  $Z = 10$  macroions [21]. They also find a two phase region on lowering temperature, with a critical point located at  $\phi \approx 0.17$  and  $\sigma/(Zl_B) \approx 0.077$ . Whilst the phenomenology is the same, the numerical values are somewhat different from the prediction of Eq. (6). Not unexpectedly, the present model is too crude to obtain quantitatively reliable results. An analogy can be made with the application of Debye-Hückel theory to the restricted primitive model (RPM) [23, 25, 48]. In this case too, Debye-Hückel theory correctly suggests a region of phase separation at low temperatures but errs in terms of quantitative predictions. Interestingly, in terms of accuracy of prediction, the present theory is not much worse than symmetrised Poisson-Boltzmann theory or the mean spherical approximation [13, 19, 49].

I now turn the effect of added salt, and analyse the predictions of the full free energy in Eq. (5). In general, as salt is added, the critical point in Fig. 1(a) first moves to higher dimensionless temperatures, passes through a maximum, and then starts to move to lower dimensionless temperatures again. This non-monotonic behaviour is shown in Fig. 1(b) for  $Z = 10^3$ . A similar effect of added salt is seen in a number of other approaches

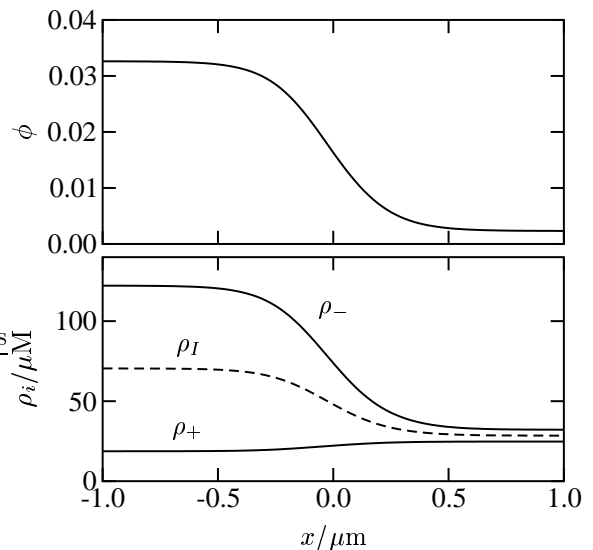


FIG. 3: Macroion volume fraction (top) and small ion concentrations (bottom) through the interface corresponding to the dashed tie line in Fig. 2.

[4, 5, 40, 50, 51, 52]. In the presence of added salt, it is no longer true that the dependence on  $Z$  and  $\sigma/l_B$  can be combined into a single parameter, however for comparison with the phase behaviour in the absence of salt, Fig. 1(b) shows the behavior as a function of  $\sigma/(Zl_B)$  at this fixed value of  $Z$ .

The re-entrant behaviour means that for parameters such as those corresponding to the dashed line in Fig. 1(b), there are *two* critical points in the  $(\rho_m, \rho_s)$  plane, and one encounters a re-entrant single phase region at low added salt. The dashed line in Fig. 1(b) is for  $Z = 10^3$ ,  $\sigma = 100$  nm and  $l_B = 0.72$  nm, and the corresponding phase behaviour in the  $(\rho_m, \rho_s)$  plane is shown in Fig. 2. It is seen that the two phase region appears as a miscibility gap in this representation.

As  $\sigma/l_B$  is increased or  $Z$  is decreased, the two critical points move towards each other and finally disappear at a double critical point, or hypercritical point [53]. For example, for  $Z = 10^3$  the double critical point corresponds to the maximum of the solid line in Fig. 1(b), where  $\sigma/(Zl_B) \approx 0.145$ ,  $\phi \approx 1.04 \times 10^{-2}$  and  $\rho_s \approx 8.98$   $\mu\text{M}$ .

The bulk phase behaviour predicted by Eq. (5) thus closely resembles that predicted by various other approaches, including the theory discussed in Ref. [5]. Many approaches, including the present one, do not consider the formation of ordered phases (colloidal crystals). These can arise from the strong macroion-macroion interactions. The possibility of ordered phases has been considered by van Roij and coworkers [4, 17, 40] though. They find that ordered phases can appear in the vicinity of the miscibility gap in which case a richer phase behaviour can result.

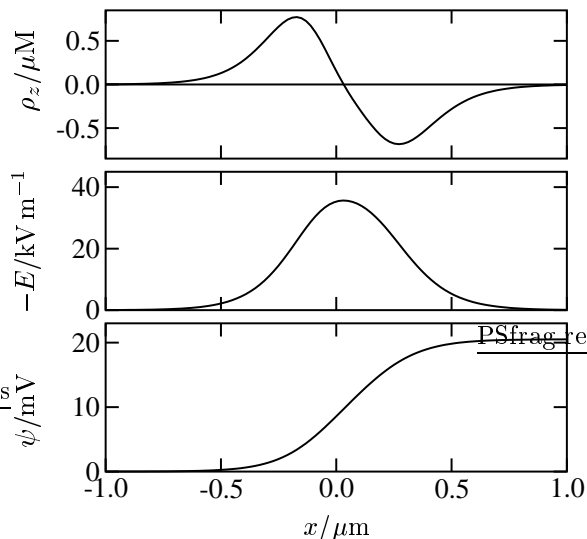


FIG. 4: Charge density (top), electric field (middle), and electrostatic potential (bottom) corresponding to the ion density profiles shown in Fig. 3.

#### IV. INTERFACIAL PROPERTIES

A major use of the density functional theory in the present context is to calculate the macroion and small ion density profiles through the interface between two coexisting phases, and to compute the surface tension. In order to set the problem up, it is convenient to introduce the grand potential [38]

$$\Omega = F - \int d^3\mathbf{r} \sum_{i=m,\pm} \mu_i \rho_i(\mathbf{r}) \quad (7)$$

where  $\mu_i$  are the chemical potentials of the three species, and  $F$  is defined in Eqs. (1)–(4). At this point it is also convenient to rewrite the mean field term in Eq. (1). Define a dimensionless electrostatic potential

$$\psi(\mathbf{r}) = l_B \int d^3\mathbf{r}' \frac{\rho_z(\mathbf{r}')}{|\mathbf{r} - \mathbf{r}'|} \quad (8)$$

so that the mean field term in Eq. (1) can be written

$$\frac{l_B}{2} \int d^3\mathbf{r} d^3\mathbf{r}' \frac{\rho_z(\mathbf{r})\rho_z(\mathbf{r}')}{|\mathbf{r} - \mathbf{r}'|} = \frac{1}{2} \int d^3\mathbf{r} \psi(\mathbf{r}) \rho_z(\mathbf{r}). \quad (9)$$

By direct substitution, one verifies that the potential defined by Eq. (8) solves the Poisson equation

$$\nabla^2 \psi + 4\pi l_B \rho_z = 0. \quad (10)$$

Using this and Green's first identity [54], the mean field term now becomes

$$\frac{1}{2} \int d^3\mathbf{r} \psi(\mathbf{r}) \rho_z(\mathbf{r}) = \frac{1}{8\pi l_B} \int d^3\mathbf{r} |\nabla \psi|^2. \quad (11)$$

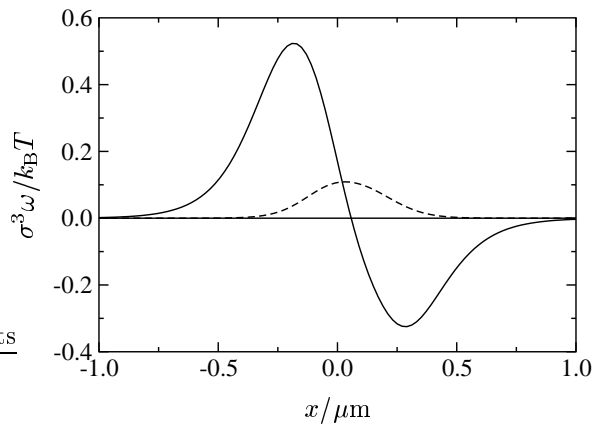


FIG. 5: Excess grand potential density (solid line) and electrostatic component thereof (dashed line) corresponding to the ion density profiles shown in Fig. 3.

This is recognised as the electric field energy since  $\nabla\psi$  is essentially the electric field strength. One can now define a grand potential density  $\omega(\mathbf{r})$  such that  $\Omega = \int d^3\mathbf{r} \omega(\mathbf{r})$  and

$$\omega = \sum_i \rho_i \left( k_B T \ln \frac{\rho_i}{e \rho_i^\ominus} - \mu_i \right) + \frac{k_B T}{8\pi l_B} |\nabla \psi|^2 + f_m \rho_m \quad (12)$$

where the explicit dependence on the spatial co-ordinate has been suppressed. For a homogeneous system,  $\omega = -p$  where  $p$  is the pressure.

Setting  $\delta\Omega/\delta\rho_i(\mathbf{r}) = 0$  and using Eq. (8) gives

$$\begin{aligned} \frac{\mu_i}{k_B T} &= \ln \frac{\rho_i(\mathbf{r})}{\rho_i^\ominus} + z_i \psi(\mathbf{r}) \\ &+ \frac{\delta}{\delta\rho_i(\mathbf{r})} \left( \frac{\int d^3\mathbf{r}' \rho_m(\mathbf{r}') f_m(\mathbf{r}')}{k_B T} \right). \end{aligned} \quad (13)$$

In principle, these non-linear integral equations can be solved to find the ion density profiles. Here a variational approximation has been adopted in which  $\Omega$  is minimised with respect to parameters in trial functions which specify the ion density profiles. More details of the numerical approach are given in Appendix B.

I now suppose that all the variation occurs in one direction  $x$  normal to the interface. At large distances from the interface,  $x \rightarrow \pm\infty$ , the number densities approach those corresponding to the coexisting bulk phases. The grand potential density approaches a constant value  $\omega(\pm\infty)$  equal to (minus) the pressure, and therefore the same in coexisting phases. The surface tension  $\gamma$  can therefore be identified as the excess grand potential per unit area

$$\gamma = \int_{-\infty}^{\infty} dx [\omega - \omega(\pm\infty)]. \quad (14)$$

The chemical potentials derived from Eq. (5) are

$$\frac{\mu_i}{k_B T} = \ln \frac{\rho_i}{\rho_i^\ominus} + z_i \psi + \frac{\partial}{\partial\rho_i} \left( \frac{2Z^2 l_B \rho_m}{\sigma(\sigma\kappa + 2)} \right). \quad (15)$$

Comparison with Eq. (13) shows that  $\psi$  in this expression is simply the limiting value of  $\psi(\mathbf{r})$  in the case of a homogeneous system [55]. For the interface problem, one has two limiting values,  $\psi(\pm\infty)$ . The difference  $\Delta\psi = \psi(\infty) - \psi(-\infty)$  arises because of the electrical structure at the interface. It is a liquid-liquid junction potential analogous to the Donnan potential that appears across a semi-permeable membrane [56]. Since  $\psi$  in Eq. (15) is determined by the bulk densities, the difference  $\Delta\psi$  can be calculated without having to solve for the interface structure. In fact, because of the symmetric way that  $\rho_{\pm}$  enters into the excess free energy, a simple expression obtains,

$$\Delta\psi = \frac{1}{2} \ln \left( \frac{\rho_{-}(\infty)}{\rho_{+}(\infty)} \cdot \frac{\rho_{+}(-\infty)}{\rho_{-}(-\infty)} \right). \quad (16)$$

This method of calculating the junction potential was used in Ref. [5].

One question remains: what should be used for the chemical potentials in these calculations? The simplest answer is to compute the chemical potentials from Eq. (15), setting  $\psi = 0$  and using the bulk densities corresponding to either one of the coexisting phases. This works because global charge neutrality means Eq. (14) for the surface tension is unaffected by the value of  $\psi$  in Eq. (15). Hence we are free to set  $\psi = 0$  in either of the coexisting phases.

I now turn to the results. Fig. 3 shows representative density profiles for the macroion and small ions through the interface between the coexisting phases, corresponding to the highlighted tie line in Fig. 2. The profiles interpolate smoothly between the coexisting bulk densities. Fig. 4 shows the detailed electrical structure at the interface. The upper plot shows that the charge density  $\rho_z = Z\rho_M + \rho_+ - \rho_-$  has a dipolar structure. Correspondingly there is a localised electric field, shown in the middle plot, and a smooth jump of  $\Delta\psi \approx 20.5$  mV in the electrostatic potential, shown in the lower plot. This is the junction potential which can also be calculated directly from the coexisting bulk densities as in Eq. (16). This electrical structure is in accord with general expectations for charged systems [45, 57].

Fig. 5 shows the grand potential density and the electrostatic component thereof—the second term of Eq. (12)—as a function of distance through the interface. For this particular case the area gives  $\gamma \approx 0.727 \times (k_B T / \sigma^2)$ . The order of magnitude of this should not come as a surprise since  $\sigma$  and  $k_B T$  are the only relevant length and energy scales in the problem. Inserting actual values,  $\gamma \sim 0.3 \mu\text{N m}^{-1}$ , which is typical for soft matter interfaces [31].

Fig. 6 shows how the surface tension and interface width vary as one approaches the upper critical point in Fig. 2. The width  $d$  is defined operationally as  $d^2 = \langle x^2 \rangle - \langle x \rangle^2$ , where  $\langle \dots \rangle = \int_{-\infty}^{\infty} (\dots) p(x) dx / \int_{-\infty}^{\infty} p(x) dx$ , with  $p(x) = |\omega(x) - \omega(\pm\infty)|^2$ . These results are obtained by repeating the calculations underlying Figs. 3–5 for a sequence of tie lines approaching the critical point. They

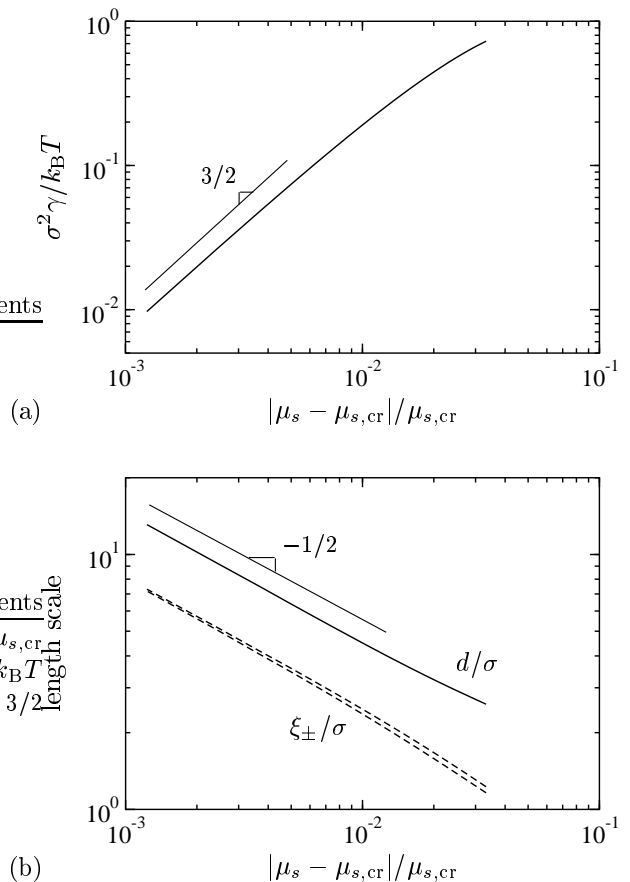


FIG. 6: (a) Surface tension as a function of salt chemical potential. (b) Interface width (solid line) and correlation lengths (dashed lines) as a function of salt chemical potential. In both, the salt chemical potential is expressed as a normalised distance from the upper critical point.

are reported as a function of the distance from the critical point, expressed in terms of a normalised salt chemical potential. Fig. 6(b) also shows the correlation lengths  $\xi_{\pm}$  in the coexisting phases determined from the exponential decay of the density profiles into the bulk phases (see Appendix B). As the critical point is approached, these approach each other, and diverge in the same way as the interface width. Fig. 6 reveals that the surface tension and length scales are in accord with expected scaling behaviour for a mean-field theory [58].

What happens at the lower critical point in Fig. 2 though? The next section shows that this is a non-trivial question with perhaps an unexpected answer. In the calculations in the current section, I have assumed that the interface profiles smoothly interpolate between the coexisting phases. Indeed, this is the basis of the numerical method detailed in Appendix B. However, such an approach rules out the possibility of oscillatory behaviour in the density profiles (or to be precise, the numerical methodology is inappropriate for this scenario). At lower salt concentrations though, one can enter a region where

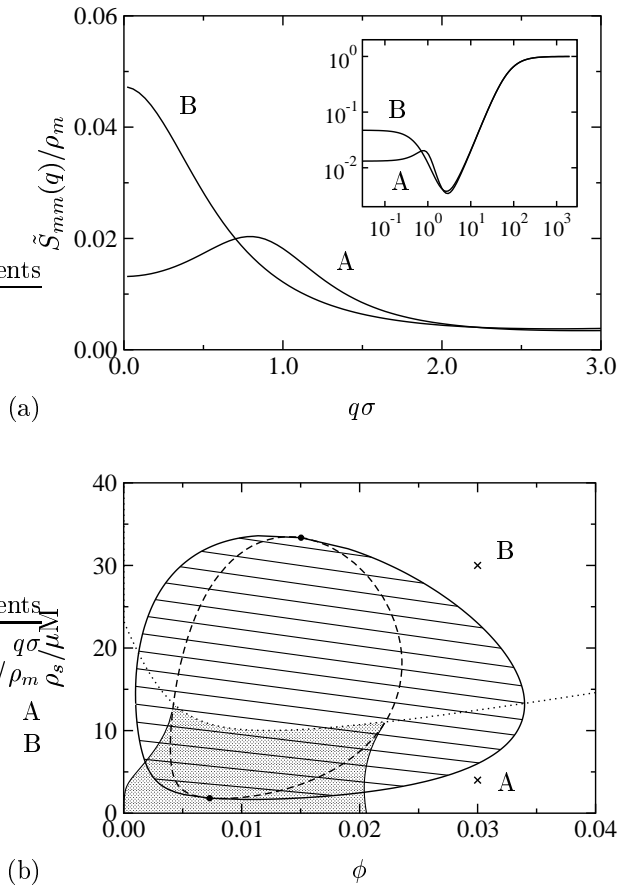


FIG. 7: (a) Macroion structure factors at  $\phi = 0.03$ , and  $\rho_s = 4 \mu\text{M}$  (A) and  $30 \mu\text{M}$  (B). The inset shows the same curves in a double-logarithmic plot. The normalisation is such that  $\tilde{S}_{mm}/\rho_m \rightarrow 1$  as  $q \rightarrow \infty$ . (b) Phase diagram augmented by the spinodal line (dashed), the Lifshitz line (dotted), and the region where the macroion structure factor diverges at a non-zero wavevector (shaded).

oscillatory behaviour is expected. These considerations are made mathematically precise in the next section.

## V. STRUCTURE FACTORS

The structure factors in a homogeneous system can be determined from a density functional theory (DFT) by functional differentiation [38]. Where accurate structure factors are already known, typically from a combination of simulation and integral equation approaches, this can be used to constrain the DFT. In the present case for example, one could try to constrain  $w(r)$  in Eq. (4). However accurate structure factors are not known for this problem, and furthermore the DFT has been constructed to include only the macroion self energy. Thus it does not make sense to constrain the DFT and the present section simply reports the structure factors that are predicted from the theory as given in Eqs. (1)–(4).

The structure factor matrix is [59, 60]

$$\tilde{S}_{ij}(q) = \rho_i \delta_{ij} + \rho_i \rho_j \tilde{h}_{ij}(q) \quad (17)$$

where  $i$  and  $j$  run over  $\{m, +, -\}$  and  $\tilde{h}_{ij}(q) = \int d^3\mathbf{r} e^{-i\mathbf{q}\cdot\mathbf{r}} h_{ij}(r)$  is the Fourier transform of the pair correlation functions  $h_{ij}(r) = g_{ij}(r) - 1$ . Reciprocal space quantities will be denoted by a tilde. The bulk densities  $\rho_i$  are constants, fixed by the choice of state point. Deviations away from these will be denoted by  $\Delta\rho_i$ . Eq. (17) uses the normalisation  $\tilde{S}_{ij}(q) \rightarrow \rho_i \delta_{ij}$  as  $q \rightarrow \infty$ , which simplifies some of the expressions below [60].

To obtain the structure factor matrix, start by defining the real-space function

$$S_{ij}^{-1}(|\mathbf{r} - \mathbf{r}'|) = \frac{1}{k_B T} \left( \frac{\delta^2 F}{\delta\rho_i(\mathbf{r})\delta\rho_j(\mathbf{r}')} \right)_{\rho_i(\mathbf{r}) \rightarrow \rho_i} \quad (18)$$

where  $F$  is the full free energy. The limit of a homogeneous system is taken after the functional differentiation step so that  $S_{ij}^{-1}$  only depends on  $|\mathbf{r} - \mathbf{r}'|$  as indicated. Transforming to reciprocal space, one can show that

$$\tilde{S}_{ij}^{-1}(q) = \int d^3\mathbf{r} e^{-i\mathbf{q}\cdot\mathbf{r}} S_{ij}^{-1}(r) \quad (19)$$

is simply the matrix inverse of  $\tilde{S}_{ij}$ ,

$$\sum_j \tilde{S}_{ij} \tilde{S}_{jk}^{-1} = \delta_{ik}. \quad (20)$$

These results follow by combining the Ornstein-Zernike relation for a multicomponent mixture in reciprocal space,  $\tilde{h}_{ij} = \tilde{c}_{ij} + \sum_k \rho_k \tilde{c}_{ik} \tilde{h}_{jk}$  where  $c_{ij}$  are the direct correlation functions [59], with the DFT result that  $c_{ij} = -(1/k_B T) \delta^2 F_{\text{ex}} / \delta\rho_i \delta\rho_j$  where  $F_{\text{ex}}$  is the excess free energy [38].

The route to the structure factors offered by Eqs. (18)–(20) is based on ‘classical’ arguments [59]. One can also make the connection via field theoretical methods. Expanding the free energy functional to second order gives

$$\frac{\Delta F}{k_B T} = \frac{1}{2} \int d^3\mathbf{r} d^3\mathbf{r}' \sum_{ij} \Delta\rho_i(\mathbf{r}) \Delta\rho_j(\mathbf{r}') S_{ij}^{-1}(|\mathbf{r} - \mathbf{r}'|), \quad (21)$$

where  $S_{ij}^{-1}$  is defined by Eq. (18). It follows that [61]

$$\langle \Delta\rho_i(\mathbf{r}) \Delta\rho_j(\mathbf{r}') \rangle = S_{ij}(|\mathbf{r} - \mathbf{r}'|) \quad (22)$$

where  $S_{ij}(r) = \int d^3\mathbf{q} / (2\pi)^3 e^{i\mathbf{q}\cdot\mathbf{r}} \tilde{S}_{ij}(q)$  is the structure factor matrix expressed as a real space quantity. Although care has to be taken at the point  $\mathbf{r} = \mathbf{r}'$ , one can easily show that the density-density correlation function on the left hand side of Eq. (22) is the same as the Fourier transform of the right hand side of Eq. (17).

The Stillinger-Lovett moment conditions constrain the behaviour of the structure factors in reciprocal space in a particularly clear manner [33, 34, 44, 62, 63]. Firstly, the zeroth-moment conditions express perfect screening and are  $\int d^3\mathbf{r} \sum_i z_i \rho_i g_{ij}(r) = -z_j$  for  $j = \{m, +, -\}$ . Using

charge neutrality and assuming the structure factors are regular at  $q = 0$ , one can easily show that this implies

$$\sum_i z_i \tilde{S}_{ij}(\mathbf{q}) = O(q^2). \quad (23)$$

The second-moment condition is  $\int d^3\mathbf{r} r^2 \sum_{ij} z_i z_j \rho_i \rho_j g_{ij}(r) = -3/(2\pi l_B)$ . This constrains the long wavelength behaviour of the charge-charge structure factor,

$$\sum_{ij} z_i z_j \tilde{S}_{ij}(\mathbf{q}) = \frac{q^2}{(4\pi l_B)} + O(q^4). \quad (24)$$

In real space, this means that  $\langle \Delta\rho_z(\mathbf{r})\Delta\rho_z(\mathbf{r}') \rangle \sim l_B/|\mathbf{r} - \mathbf{r}'|$  for  $|\mathbf{r} - \mathbf{r}'| \rightarrow \infty$ . Thus charge density fluctuations vanish with the Coulomb law at large distances, corresponding to the fact that the electrostatic energy dominates in the free energy for long-wavelength density fluctuations unless they happen to be charge-neutral [64].

I now apply the formalism of Eqs. (18)–(20) to the present DFT defined in Eqs. (1)–(4). The result for the inverse structure factor matrix in reciprocal space can be written as

$$\tilde{S}_{ij}^{-1} = \tilde{T}_{ij}^{-1} + \frac{4\pi l_B z_i z_j}{q^2} \quad (25)$$

where first term comes from the ideal and correlation contributions to the free energy and the second term from the mean field electrostatics. The first term is in detail

$$\begin{aligned} \tilde{T}_{ij}^{-1} = & \delta_{ij}/\rho_i + \rho_m Z^2 \pi^2 l_B^3 \sigma^3 h_1(\sigma\kappa, \sigma q) \Delta'_{ij} \\ & - Z^2 \pi l_B^2 \sigma h_2(\sigma\kappa, \sigma q) \Delta''_{ij}. \end{aligned} \quad (26)$$

where the functions  $h_{1,2}(x = \sigma\kappa, y = \sigma q)$  are

$$h_1 = \frac{8e^{-\alpha y^2/2}(2+3x)}{(x^3(x+2)^3)}, \quad h_2 = \frac{4e^{-\alpha y^2/4}}{(x(x+2)^2)}, \quad (27)$$

and the matrices are

$$\begin{aligned} \Delta'_{mm} = \Delta'_{m\pm} = 0, \quad \Delta'_{\pm\pm} = 1, \\ \Delta''_{mm} = \Delta''_{\pm\pm} = 0, \quad \Delta''_{m\pm} = 1. \end{aligned} \quad (28)$$

The  $y$ -dependence ( $y = \sigma q$ ) in Eq. (27) arises from the Fourier transform of the weight function of Eq. (4). Note that the point model alluded to in section II corresponds to the limit  $\alpha \rightarrow 0$  in Eqs. (27). In this limit, the theory becomes ill-defined since  $\tilde{S}_{ij}(q)$  does not have the correct limiting behaviour as  $q \rightarrow \infty$ . This was the original technical reason for introducing the smoothing kernel.

For any given state point and value of  $q$ , Eqs. (25)–(28) define  $\tilde{S}_{ij}^{-1}$  which can be inverted numerically to find all components of the structure factor matrix. A partial solution can be obtained analytically in terms of the subsidiary matrix  $\tilde{T}_{ij}$ ,

$$\tilde{S}_{ij} = \tilde{T}_{ij} - \frac{4\pi l_B \sum_{kl} z_k z_l \tilde{T}_{ik} \tilde{T}_{jl}}{q^2 + 4\pi l_B \sum_{kl} z_k z_l \tilde{T}_{kl}} \quad (29)$$

From this one can readily prove that  $\tilde{S}_{ij}$  exactly satisfies the Stillinger-Lovett moment conditions in Eqs. (23) and (24) above.

Another result follows from the dominance of the ideal contribution over the correlation contribution at low densities. In the limit  $\rho_i \rightarrow 0$  one finds  $\tilde{T}_{ij} \rightarrow \rho_i \delta_{ij}$  and

$$\tilde{S}_{ij} \rightarrow \rho_i \delta_{ij} - \frac{4\pi l_B z_i z_j \rho_i \rho_j}{q^2 + 4\pi l_B \sum_k z_k^2 \rho_k}. \quad (30)$$

This is in fact exactly in accordance with the Debye-Hückel limiting law at low densities. To see this, note that  $\lambda = (4\pi l_B \sum_k z_k^2 \rho_k)^{-1/2}$  is the Debye screening length defined to include *all* ionic species. Thus in real space, Eqs. (17) and (30) indicate that  $h_{ij} = -z_i z_j (l_B/r) e^{-r/\lambda}$ , in correspondence with the Debye-Hückel limiting law.

It is clear that the moment conditions and the Debye-Hückel limiting law behaviour follow from the construction of the DFT to include a mean-field contribution separately from the correlation term. This construction is in turn motivated by the expected behaviour of the direct correlation functions  $c_{ij}(r)$  at  $r \rightarrow \infty$ , as Evans and Sluckin have described [44]. The form of the correlation term is unimportant, so long as it is regular both at  $q \rightarrow 0$  and  $\rho_i \rightarrow 0$ .

For the remaining part, I now focus on the macroion structure factor  $\tilde{S}_{mm}$ . Note that the theory includes the macroion-macroion electrostatic interaction explicitly in the mean field term, and an additional indirect interaction in the correlation term. The computation of  $\tilde{S}_{mm}$  reveals the combined effect of these macroion *interactions* on the macroion *correlations*.

Typically  $\tilde{S}_{mm}$  has a ‘hole’ in reciprocal space for  $q\sigma \lesssim 1$ . This corresponds to the macroion electrostatic repulsions. Within the correlation hole though, there is additional structure. This becomes particularly important in the vicinity of the phase separation region. Two kinds of behaviour are possible: at higher salt concentrations  $\tilde{S}_{mm}$  rises to a maximum as  $q \rightarrow 0$ , or at lower salt concentrations  $\tilde{S}_{mm}$  acquires a peak at some  $q^* > 0$ . In the phase diagram, the two alternatives are separated by a (macroion) ‘Lifshitz line’ [65], defined to be the locus of points for which  $\partial\tilde{S}_{mm}/\partial(q^2)|_{q=0} = 0$ . Fig. 7(a) shows the two behaviours for a pair of typical state points above and below the Lifshitz line, and Fig. 7(b) shows the Lifshitz line superimposed on the bulk phase behaviour.

Also shown in Fig. 7(b) is the spinodal line computed from the bulk free energy in Eq. (5) of section III. One can check that  $\tilde{S}_{mm}(q=0)$  diverges on this spinodal line; in fact all the  $q=0$  components of the structure factor matrix diverge because the determinant of  $\tilde{S}_{ij}^{-1}$  vanishes. For salt concentrations above the Lifshitz line, this divergence at  $q=0$  can be accommodated within the general behaviour of the structure factor. Of course, state points within the binodal are metastable so the divergence is strictly only visible as the upper critical point is approached. The fact that the structure factors diverge

on the spinodal line is no coincidence, since thermodynamic consistency by the compressibility route is assured for a DFT [66].

What happens at salt concentrations below the Lifshitz line? Here, the peak in  $S_{mm}$  at  $q^* > 0$  is found to diverge *before* the bulk spinodal line is reached. The shaded area in Fig. 7(b) shows the region where this occurs. A divergence at a non-zero wavevector is indicative of microphase separation [67]. In this case one would expect a charge-density-wave (CDW) phase to appear [36, 68]. The shaded region extends below the binodal for bulk phase separation, so the CDW phase should be observable in this part of the phase diagram. In fact the CDW phase will be found whenever the lower critical point lies below the Lifshitz line. The general idea that a critical point in a charged system can be replaced by a CDW phase was advanced by Nabutovskii, Nemov and Peisakhovich [36, 69].

The location of the Lifshitz line depends on the parameter  $\alpha$  which sets the range of the smoothing kernel  $w(r)$  in Eq. (4). If  $\alpha \lesssim 0.40$  the Lifshitz line moves upwards past the upper critical point, which would then be expected to be replaced by a CDW phase too. On the other hand if  $\alpha \gtrsim 3.6$ , the Lifshitz line moves downwards past the lower critical point. These critical values of  $\alpha$  only depend on the coefficient of  $q^2$  in the expansion of the Fourier transform of  $w(r)$  about  $q = 0$ .

The Lifshitz line discussed here pertains to the macroion structure factor. Although slightly different Lifshitz lines are expected for each component of the structure factor matrix, the locus of state points where the peak diverges (either on the spinodal or on the boundary of the CDW phase) should be the same for all components.

Whilst the Lifshitz line marks an obvious change in the behaviour of  $\tilde{S}_{mm}$ , the cross-over from monotonic to damped oscillatory asymptotic decay of the correlation functions  $h_{ij}(r)$  is determined by Kirkwood or Fisher-Widom lines in the phase diagram [70, 71, 72]. The difference between these is rather subtle [72, 73], and one might loosely cover both possibilities by the phrase ‘Kirkwood-Fisher-Widom’ (KFW) line. The importance of the KFW line lies in the fact that it also governs the asymptotic decay of the interface density profiles, which behave in the same way as  $h_{ij}$  [71]. Thus the calculations reported in section IV above, which assume that there is no oscillatory behaviour in the density profiles, requires as a necessary minimum that the coexisting bulk densities both lie above the KFW line. The location of the KFW line is governed by the poles of  $\tilde{S}_{ij}(q)$  in the complex  $q$  plane, which are either purely imaginary or occur as complex conjugate pairs, and are the same for all components of  $\tilde{S}_{ij}$  [71]. If the pole nearest the real  $q$ -axis is purely imaginary, then monotonic decay is expected; conversely if a pair of complex conjugate poles is nearest the real  $q$ -axis, then damped oscillatory decay is expected [72]. Determination of the KFW line is a hard numerical problem and has not been attempted for the

present DFT. However the presence of a peak in  $\tilde{S}_{mm}(q)$  on the real  $q$ -axis at  $q = 0$ , or at  $q^* > 0$ , ought to be indicative of whether the pole nearest the real  $q$ -axis is, or is not, purely imaginary. Thus the Lifshitz line should serve as a guide to the location of the KFW line. In section IV therefore, care was taken to make sure that the coexisting bulk densities lie well above the Lifshitz line.

## VI. DISCUSSION

The paper presents a density functional theory (DFT) for a macroion suspension. The excess free energy corresponds to the macroion self energy evaluated using Debye-Hückel theory. These approximations render theory tractable without losing the basic phenomenology which resembles that of other studies. The advantage of a DFT is that one can compute the interface structure and surface tension between coexisting phases. The results are in accord with expectations from previous work [5]. In particular, the electrical structure of the interface gives rise to a junction potential analogous to the Donnan potential across a semi-permeable membrane. This arises from an electric dipole moment density (per unit area of interface), which appears because charge neutrality is locally violated in the vicinity of the interface. The surface tension is found to be of the order  $k_B T / \sigma^2$ .

Structure factors can be computed from the DFT. These are found to obey the Stillinger-Lovett moment conditions, although this is not a stringent test of the theory. The structure factors reveal an interesting phenomenon, namely that oscillatory behaviour can appear in the (direct) correlation functions, particularly at low ionic strength. Indeed there may be regions of microphase separation in the vicinity of the critical points, corresponding to the appearance of a charge-density-wave (CDW) phases. This phenomenon is peculiar to asymmetric charged systems [36], and is strictly absent in symmetric systems such as the restricted primitive model. In this respect, the possibility of CDW phases is correlated with the appearance of the junction potential, which is also strictly absent in symmetric systems [35]. Given the approximate nature of the DFT, only certain aspects of the present analysis might be expected to survive in a full treatment. One of these is an upturn in macroion structure factor at small  $q$ , even in the absence of a true miscibility gap. This would reflect an increased osmotic compressibility in this region of the phase diagram. Another expectation is the possible appearance of the CDW phases, although it might be difficult to disentangle these from the ordered (crystal) phases that are expected for a macroion suspension at sufficiently strong electrostatic coupling.

The macroion self energy depends on the local ionic strength, but on both physical and technical grounds it is found necessary to introduce the notion of smoothing or smearing—the dependency should be on the ionic strength averaged over the vicinity of the macroion. Here

a completely phenomenological approach has been taken to construct the details of the DFT. Other choices could be made, or indeed more rigor could be introduced, such as additional requirements for internal consistency [74]. Tests indicate though that the general phenomenology (electrical structure of interface, gross behaviour of structure factors) is found to be insensitive to the details of the model at this point.

### Acknowledgments

I thank R. Evans and A. S. Ferrante for useful discussions.

### APPENDIX A: CORRECTION TO REF. [5]

Chan [6] has remarked that an excluded volume contribution was omitted in the theory of Ref. [5]. This appendix describes the missing term. The error occurs in going from Eq. (3) to Eq. (7) of Ref. [5] where the omitted contribution arises from the fact that  $h_{m\pm}(r) = g_{m\pm}(r) - 1 = -1$  for  $r < \sigma/2$ . In terms of the microion-macroion interaction energy,  $E_{ms}/(Vk_B T)$ , the omitted contribution is

$$\begin{aligned} & \rho_m \int_{|\mathbf{r}| < \sigma/2} d^3\mathbf{r} \frac{Zl_B}{r} [\rho_+ h_{m+}(r) - \rho_- h_{m-}(r)] \\ &= -\rho_m(\rho_+ - \rho_-) \int_0^{\sigma/2} 4\pi r^2 dr \frac{Zl_B}{r} \\ &= +\frac{\pi Z^2 l_B \rho_m^2 \sigma^2}{2} \quad (\text{using } \rho_+ - \rho_- = -Z\rho_m). \end{aligned} \quad (\text{A1})$$

This contribution is a positive, increasing function of  $\rho_m$ , and has the tendency to stabilise the system against phase separation (because it is an athermal excluded volume term, it passes unscathed through the thermodynamic integration step needed to calculate the contribution to the free energy). If the calculations of Ref. [5] are repeated with this contribution included, it is found that the miscibility gap in the  $(\rho_m, \rho_s)$  plane does not appear until somewhat larger values of  $Zl_B/\sigma$ . Fig. 8 shows the new results in comparison with those reported in Table II of Ref. [5]. The new calculation indicates that phase separation is observed in an even narrower window of parameter space for which the Debye-Hückel linearisation approximation might be admissible than was found in the earlier work. This can be taken to indicate that the self-energy mechanism may not be sufficiently powerful to drive phase separation by itself, as discussed in the introduction.

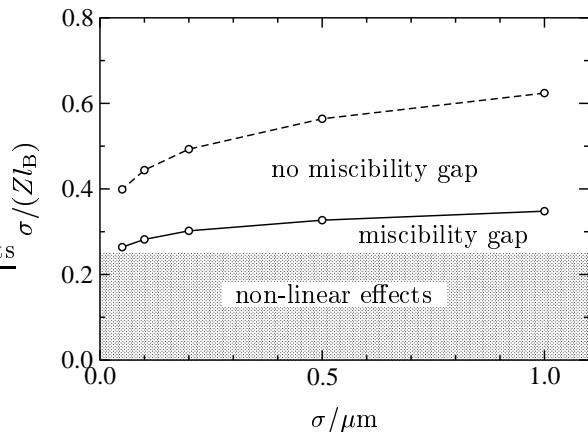


FIG. 8: State diagram showing where a miscibility gap is found for the full theory of Ref. [5] including the omitted term (solid line), compared to the original results (dashed line). The shaded region shows where  $Z \gtrsim 4\sigma/l_B$ , which is one possible criterion for the acceptability of the Debye-Hückel approximation for the polarisation energy [5].

### APPENDIX B: NUMERICAL APPROACH

The task is to find density profiles  $\rho_i(x)$  which minimise the grand potential in Eq. (7). The most accurate method is to solve the integral equations for the profiles in Eq. (13). However, this is hard. An alternative is to adopt a variational approach in which  $\Omega$ , or  $\gamma$  in practice, is minimised with respect to parameters in trial functions which specify the density profiles [75]. This is the approach that has been taken here.

The ion density profiles have to satisfy a sum rule since the potential difference  $\Delta\psi = \psi(\infty) - \psi(-\infty)$  is fixed by the coexisting bulk densities as described in section IV. One can replace one of the ion density profiles by  $\psi(x)$  to ensure this sum rule is automatically satisfied. In the present case, a choice was made to use the set  $\{\rho_m, \rho_+, \psi\}$  as a basis with  $\rho_-$  derived analytically from the Poisson equation,  $\rho_- = Z\rho_m + \rho_- - (d^2\psi/dx^2)/(4\pi l_B)$ . The first integral of the Poisson equation shows that one can additionally ensure global charge neutrality by making sure that  $d\psi/dx \rightarrow 0$  as  $|x| \rightarrow \infty$ . Once the  $\rho_i$  are known, the average ionic strength  $\bar{\rho}_I$  and the surface tension  $\gamma$  are determined numerically by quadratures.

To represent the basis set  $\{\rho_m, \rho_+, \psi\}$ , three copies of the function

$$\begin{aligned} f(x; \xi_{\pm}, \{a\}) &= \frac{a_- e^{x/\xi_+} - a_+ e^{-x/\xi_-}}{a_- a_+ + a_- e^{x/\xi_+} + a_+ e^{-x/\xi_-}} \\ &+ \sum_{r=1}^N a_r H_r(x/\xi) \end{aligned} \quad (\text{B1})$$

are introduced. In this, the  $H_r$  are Hermite functions, with  $\xi = 2/(1/\xi_- + 1/\xi_+)$  used to scale the argument. Each copy of  $f$  is parametrised by the correlation lengths  $\xi_{\pm}$  and amplitude set  $\{a\}$ , and has the properties that  $f \rightarrow \pm(1 - a_{\pm} e^{\mp x/\xi_{\pm}})$  as  $x \rightarrow \pm\infty$ . One copy of  $f$  is

assigned to each member of  $\{\rho_m, \rho_+, \psi\}$ , and is scaled and shifted to match the limiting values at  $|x| \rightarrow \infty$ , for example  $\rho_m = \rho_m(-\infty)(1-f)/2 + \rho_m(\infty)(1+f)/2$  (for the electrostatic potential, one can set  $\psi(-\infty) = 0$  and  $\psi(\infty) = \Delta\psi$ ). The three copies of  $f$  have different amplitude sets  $\{a\}$  but share common values for  $\xi_{\pm}$  since the asymptotic decay of the density profiles into the bulk phases is expected to be governed by a bulk correlation length—it is these values of  $\xi_{\pm}$  that are reported in Fig. 6(b). A finite set of  $N$  Hermite functions has been included in each copy of  $f$  to allow for an arbitrary structure at the interface. In practice the minimisation problem is well behaved only if the density profiles smoothly interpolate between the bulk values, for which case typically  $N = 3-6$  Hermite functions are needed to achieve convergence in  $\gamma$  to an accuracy of the order 1%. At this point, the interface problem has been reduced to a multivariate minimisation over the three copies of the amplitude set  $\{a\}$  plus the correlation lengths  $\xi_{\pm}$ . Numerical minimisation of  $\gamma$  with respect to these parameters is then undertaken by standard methods [76].

- 
- [1] K. Ito, H. Yoshida, and N. Ise, *Science* **263**, 66 (1994); A. E. Larsen and G. G. Grier, *Nature* **385**, 230 (1997).
- [2] F. Gröhn and M. Antonietti, *Macromol.* **33**, 5938 (2000).
- [3] R. van Roij and J.-P. Hansen, *Phys. Rev. Lett.* **79**, 3082 (1997); A. R. Denton, *J. Phys.: Condens. Matter* **11**, 10061 (1999); M. Knott and I. J. Ford, *Phys. Rev. E* **63**, 031403 (2001); K. S. Schmitz, *Phys. Rev. E* **65**, 061402 (2002).
- [4] R. van Roij, M. Dijkstra, and J.-P. Hansen, *Phys. Rev. E* **59**, 2010 (1999).
- [5] P. B. Warren, *J. Chem. Phys.* **112**, 4683 (2000).
- [6] D. Y. C. Chan, *Phys. Rev. E* **63**, 061806 (2001).
- [7] A. K. Akora and B. V. R. Tata, *Adv. Coll. Int. Sci.* **78**, 49 (1998); J.-P. Hansen and H. Löwen, *Annu. Rev. Phys. Chem.* **51**, 209 (2000); C. N. Likos, *Phys. Rep.* **348**, 267 (2001); Y. Levin, *Rep. Prog. Phys.* **65**, 1577 (2002).
- [8] L. Belloni, *J. Phys.: Condens. Matter* **12**, R549 (2000).
- [9] H. H. von Grünberg, R. van Roij, and G. Klein, *Europhys. Lett.* **55**, 580 (2001); M. Desarno and H. H. von Grünberg, *Phys. Rev. E* **66**, 011401 (2002).
- [10] M. N. Tamashiro and H. Schiessel, *J. Chem. Phys.* **119**, 1855 (2003).
- [11] A. Diehl, M. C. Barbosa, and Y. Levin, *Europhys. Lett.* **53**, 86 (2001); J.-F. Dufrêche, T. O. White, and J.-P. Hansen, *Mol. Phys.* **101**, 1741 (2003); Y. Levin, E. Trizac, and L. Bocquet, *J. Phys.: Condens. Matter* **15**, S3523 (2003); E. Trizac and Y. Levin, *Phys. Rev. E* **69**, 031403 (2004).
- [12] D. Y. C. Chan, P. Linse, and S. N. Petris, *Langmuir* **17**, 4202 (2001).
- [13] L. B. Bhuiyan and C. W. Outhwaite, *J. Chem. Phys.* **116**, 2650 (2002).
- [14] L. B. Bhuiyan and C. W. Outhwaite, *Physica A* **339**, 199 (2004).
- [15] S. N. Petris, D. Y. C. Chan, and P. Linse, *J. Chem. Phys.* **118**, 5248 (2003).
- [16] C. Russ, H. H. von Grünberg, M. Dijkstra, and R. van Roij, *Phys. Rev. E* **66**, 011402 (2002); A.-P. Hynninen, M. Dijkstra, and R. van Roij, *J. Phys.: Condens. Matter* **15**, S3549 (2003); A. R. Denton, *Phys. Rev. E* **70**, 031404 (2004).
- [17] A.-P. Hynninen, M. Dijkstra, and R. van Roij, *Phys. Rev. E* **69**, 061407 (2004).
- [18] L. Belloni, *Phys. Rev. Lett.* **57**, 2026 (1986); R. D. Groot, *J. Chem. Phys.* **94**, 5083 (1991); S. N. Petris and D. Y. C. Chan, *J. Chem. Phys.* **116**, 8588 (2002); G. Ruiz, J. A. Anta, and C. F. Tejero, *J. Phys.: Condens. Matter* **15**, S3537 (2003).
- [19] E. González-Tovar, *Mol. Phys.* **97**, 1203 (1999).
- [20] P. Linse and V. Lobaskin, *Phys. Rev. Lett.* **83**, 4208 (1999); *J. Chem. Phys.* **112**, 3917 (2000); V. Lobaskin and K. Qamhieh, *J. Phys. Chem. B* **107**, 8022 (2003).
- [21] J. Reščič and P. Linse, *J. Chem. Phys.* **114**, 10131 (2001).
- [22] C. P. Royall, M. E. Leunissan, and A. van Blaaderen, *J. Phys.: Condens. Matter* **15**, S3581 (2003). A. P. Philippe and G. H. Koenderink, *Adv. Coll. Int. Sci.* **100**, 613 (2003).
- [23] M. E. Fisher, *J. Stat. Phys.* **75**, 1 (1994).
- [24] G. Stell, *J. Stat. Phys.* **78**, 197 (1995).
- [25] E. Luijten, M. E. Fisher, and A. Z. Panagiotopoulos, *Phys. Rev. Lett.* **88**, 185701 (2002).
- [26] Y. C. Kim, M. E. Fisher, and E. Luijten, *Phys. Rev. Lett.* **91**, 065701 (2003).
- [27] M. Knott and I. J. Ford, *Phys. Rev. E* **65**, 061401 (2002).
- [28] I. Langmuir, *J. Chem. Phys.* **6**, 873 (1938).
- [29] S. Alexander, P. M. Chaikin, G. J. Morales, P. Pincus, and D. Hone, *J. Chem. Phys.* **80**, 5776 (1984); R. D. Groot, *J. Chem. Phys.* **95**, 9191 (1991); L. Belloni, *Coll. Surf. A* **140**, 227 (1998); E. Trizac, L. Bocquet, and M. Aubouy, *Phys. Rev. Lett.* **89**, 248301 (2002); L. Bocquet, E. Trizac, and M. Aubouy, *J. Chem. Phys.* **117**, 8138 (2002).
- [30] K. S. Schmitz, *Langmuir* **13**, 5849 (1997).
- [31] J. M. Brader and R. Evans, *Europhys. Lett.* **49**, 678 (2000); E. Scholten, R. Tuinier, R. H. Tromp, and H. N. W. Lekkerkerker, *Langmuir* **18**, 2234 (2002).
- [32] P. B. Warren, *J. Phys.: Condens. Matter* **15**, S3467 (2003).
- [33] F. H. Stillinger and R. Lovett, *J. Chem. Phys.* **49**, 1991 (1968).
- [34] P. A. Martin, *Rev. Mod. Phys.* **60**, 1075 (1988).
- [35] P. B. Warren, cond-mat/0006289.
- [36] V. M. Nabutovskii, N. A. Nemov, and Y. G. Peisakhovich, *Phys. Lett.* **79A**, 98 (1980).
- [37] J. S. Hoye and G. Stell, *J. Phys. Chem.* **94**, 7899 (1990).
- [38] R. Evans, *Adv. Phys.* **28**, 143 (1979); R. Evans, ch. 3 in *Fundamentals of Inhomogeneous Fluids*, ed. D. Henderson (Marcel Dekker, New York, 1992).
- [39] E. B. Smith, *Basic Chemical Thermodynamics* (Clarendon, Oxford, 1990).
- [40] R. van Roij and J.-P. Hansen, *Phys. Rev. Lett.* **79**, 3082 (1997).
- [41] B. Beresford-Smith, D. Y. Chan, and D. J. Mitchell, *J. Coll. Int. Sci.* **105**, 216 (1985).
- [42] This expression includes the bare self energy of the macroion, although this is unimportant unless the

- macroion charge is allowed to vary [50]. More complicated expressions for the self energy are available [5], but it has been checked that the use of these does not alter the basic phenomenology.
- [43] It has been checked that the phenomenology is robust with respect to the choice of  $w(r)$ .
- [44] R. Evans and T. J. Sluckin, *Mol. Phys.* **40**, 413 (1980).
- [45] T. J. Sluckin, *J. Chem. Soc. Faraday Trans. II* **77**, 1029 (1981).
- [46] R. Evans and M. Hasegawa, *J. Phys. C: Solid State Phys.* **14**, 5225 (1981); M. J. Stevens and M. O. Robbins, *Europhys. Lett.* **12**, 81 (1990); C. N. Patra and S. W. Ghosh, *Phys. Rev. E* **48**, 1154 (1993).
- [47] P. B. Warren, *J. Phys. II (France)* **7**, 343 (1997).
- [48] M. E. Fisher and Y. Levin, *Phys. Rev. Lett.* **71**, 3826 (1993).
- [49] Note the approximate constancy of  $Z\Gamma = 2Zl_B/\sigma$  at the critical points in Table V of Ref. [13].
- [50] A. Diehl, M. C. Barbosa, and Y. Levin, *Europhys. Lett.* **53**, 86 (2001).
- [51] S. N. Petris and D. Y. C. Chan, *J. Chem. Phys.* **116**, 8588 (2002).
- [52] J.-F. Duf r che, T. O. White, and J.-P. Hansen, *Mol. Phys.* **101**, 1741 (2003).
- [53] J. S. Walker and C. A. Vause, *J. Chem. Phys.* **79**, 2660 (1983).
- [54] F. A. Hinchey, *Introduction to Applicable Mathematics* (Wiley Eastern, New Delhi, 1980).
- [55] Eq. (9) limits to  $\psi\rho_z/2$  which is different from Eq. (5). This is because the constraint term in Eq. (5) is inserted by hand and does not correspond to a charging process. The difficulty is more apparent than real though, since it disappears when the chemical potentials are computed. Also note that  $\psi$  is not the true mean electrostatic potential because it ignores the electrical structure of the double layers around the macroions.
- [56] F. G. Donnan, *Z. Elektrochem.* **17**, 572 (1911); J. T. G. Overbeek, *J. Coll. Sci.* **8**, 593 (1953).
- [57] V. M. Nabutovskii and N. A. Nemov, *J. Coll. Int. Sci.* **114**, 208 (1986); B. Groh, R. Evans, and S. Dietrich, *Phys. Rev. E* **57**, 6944 (1998).
- [58] J. S. Rowlinson and B. Widom, *Molecular Theory of Capillarity* (Clarendon, Oxford, 1989).
- [59] J.-P. Hansen and I. A. McDonald, *Theory of Simple Liquids* (Academic, New York, 1976).
- [60] N. H. March and M. P. Tosi, *Atomic Dynamics in Liquids* (Macmillan, London, 1976).
- [61] M. Doi and S. F. Edwards, *The Theory of Polymer Dynamics* (Clarendon, Oxford, 1986).
- [62] J. Stafiej and J. P. Badiali, *J. Chem. Phys.* **106**, 8579 (1997).
- [63] B. P. Lee and M. E. Fisher, *Europhys. Lett.* **39**, 611 (1997).
- [64] The second-moment condition also implies that the fluid behaves as a conducting medium [34]. It may fail at a critical point; see Ref. [62] and J.-N. Aqua and M. E. Fisher, *Phys. Rev. Lett.* **92**, 135702 (2004).
- [65] A. J. Archer, C. N. Likos, and R. Evans, *J. Phys.: Condens. Matter* **14**, 12031 (2002).
- [66] One would not expect consistency by the energy or virial routes because these invoke the pair potentials. Whilst the pair potentials are of course specified in the primitive model, the DFT itself is approximate.
- [67] V. Y. Borue and I. Y. Erukhimovich, *Macromol.* **21**, 3240 (1988); J. F. Joanny and L. Leibler, *J. Phys. (France)* **51**, 545 (1990).
- [68] V. M. Nabutovskii, N. A. Nemov, and Y. G. Peisakhovich, *Mol. Phys.* **54**, 979 (1985).
- [69] When fluctuation effects are taken into account, the transition to a CDW phase is expected to become weakly first order; see S. A. Brazovskii, *Sov. Phys. JETP* **41**, 85 (1975).
- [70] J. G. Kirkwood, *Chem. Rev.* **19**, 275 (1936); M. E. Fisher and B. Widom, *J. Chem. Phys.* **50**, 3756 (1969).
- [71] R. Evans, R. J. F. Leote de Carvalho, J. R. Henderson, and D. C. Hoyle, *J. Chem. Phys.* **100**, 591 (1994).
- [72] R. J. F. Leote de Carvalho and R. Evans, *Mol. Phys.* **83**, 619 (1994).
- [73] Roughly, the period of the oscillations diverges as one approaches a Kirkwood line, but not as one approaches a Fisher-Widom line; see Ref. [72].
- [74] For example, it has not been checked that  $g_{ij}(r) \geq 0$ . Also, one could require that the  $g_{ij}(r)$  computed from the structure factors are the same as those that can be computed by solving the inhomogeneous problem of the density profiles in an appropriately chosen external potential [38]. Such requirements would introduce additional numerical complexity into the problem though.
- [75] J. R. Smith, *Phys. Rev.* **181**, 522 (1969); L. Orosz, *Phys. Rev. B* **37**, 6490 (1988).
- [76] W. H. Press, B. P. Flannery, S. A. Teucholsky, and W. T. Vetterling, *Numerical Recipes* (CUP, Cambridge, 1989).